

A Biologically Inspired Spiking Model of Visual Processing for Image Feature Detection

Dermot Kerr^{a,1}, T. M McGinnity^{a,b}, Sonya Coleman^a, Marine Clogenson^{a,2}

^aIntelligent Systems Research Centre, University of Ulster, Magee Campus, Northern Ireland

^bSchool of Science & Technology, Nottingham Trent University, Nottingham, United Kingdom

{d.kerr, sa.coleman, tm.mcginny}@ulster.ac.uk, marine.clogenson@epfl.ch

Abstract:

To enable fast reliable feature matching or tracking in scenes, features need to be discrete and meaningful, and hence edge or corner features, commonly called interest points are often used for this purpose. Experimental research has illustrated that biological vision systems use neuronal circuits to extract particular features such as edges or corners from visual scenes. Inspired by this biological behaviour, this paper proposes a biologically inspired spiking neural network for the purpose of image feature extraction. Standard digital images are processed and converted to spikes in a manner similar to the processing that transforms light into spikes in the retina. Using a hierarchical spiking network, various types of biologically inspired receptive fields are used to extract progressively complex image features. The performance of the network is assessed by examining the repeatability of extracted features with visual results presented using both synthetic and real images.

Keywords: Spiking neural networks, Image feature detection.

1. INTRODUCTION

Biological visual systems are intrinsically complex hierarchical processing systems with diverse specialised neurons, various layers and feedback loops, displaying very powerful specific biological processing functionalities that traditional computer vision techniques have not yet fully emulated. Previous research has shown that the visual system deals with visual information processing by using complicated networks of diverse specialised neurons and complex interconnections to adapt to an extensive set of dynamic visual environments (Gollisch and Meister, 2010). Existing bio-inspired artificial vision technology has neglected the possible benefit of modelling this rich diversity of cells.

In this work we present a hierarchical spiking neural network that focuses on modelling specific types of neuronal visual circuitry, in order to emulate specific aspects of a biological vision system. We develop a biologically inspired system that is capable of extracting key points from static images. Section 2 presents the background to this research. Section 3 describes the implementation of the presented model, including detailing the specific spiking neuron model used, centre-surround receptive fields, orientation specific receptive fields, end-stopped receptive fields, and full details of all the layers in the hierarchal model. Experimental results are presented in Section 4, including example visual results with synthetic images and real images, and a comprehensive performance

¹ Corresponding author: Dermot Kerr, Intelligent Systems Research Centre, University of Ulster, Magee Campus, Northern Ireland, BT48 9BL. Tel:+ 44 28716 75330. Email: d.kerr@ulster.ac.uk

² Present address: EPFL, MC B2 293, Rue de la Maladière 71b, CP 526, CH-2002 Neuchâtel 2, Switzerland.

evaluation is executed using a well-known feature repeatability evaluation technique. Section 5 discusses the network performance with advantages and weaknesses of the approach highlighted and also explores some possible areas for future improvement.

2. BACKGROUND

The retina is the only source of visual information to the brain. It is a light sensitive tissue lining within the inner surface of the eye. It is regarded as an extension of the brain and formed embryonically from neural tissue and connected to the brain by the optic nerve. Neurons within the retina are arranged in three cellular layers and are interconnected in two intervening synaptic layers. The retina is composed of approximately 50 distinct types of cells. Visual processing begins in the first cellular layer when photons stimulate the 90 million rod photoreceptors and 6 million cone photoreceptors. These cells convert the information into chemical signals and send them through intermediate networked layers of various cell types with distinct functional processing abilities. The resulting processed visual scene from this network is represented by 1.2 million retinal ganglion cells of 15 distinct types in the retina's output layer. The retinal ganglion cells convey a representation of the visual scene using action potentials (or spikes) along the ganglion cell axons to the optic nerve and onwards to the lateral geniculate nucleus and the visual cortex within the brain.

Each of the 15 distinct types of ganglion cells in the retina covers the entire visual field and transmits a completely processed image of the scene to higher brain areas (Wassle, 2004). Recent research has identified that computations of functional visual characteristics such as texture motion detection, approaching motion detection, orientation detection, contrast detection and motion extrapolation are carried out within the retina, the first stage in visual processing, and are not restricted to higher stages in the visual system as was once previously thought. Object-motion-sensitive ganglion cells in the retina, for example, have been found to distinguish between local object motion and global, self-induced motion, thus providing a rapid information channel for disentangling complex dynamical scenes. Similarly, retinal cells sensitive to approaching motion might underlie a quick avoidance reaction, and the observed retinal mechanisms for motion extrapolation are thought to underlie real-time object tracking. These insights illustrate the important role of early vision processing (i.e. retina level) in biological systems in terms of the detection of specific features, and highlight some of the advantages that a bio-inspired vision system could bring to artificial vision applications.

The detection of these specific types of features is facilitated through a number of powerful biological functionalities. For example, the diverse range of retinal and visual cortex neurons exhibit strong nonlinear processing steps and the specific connectivity between neurons incorporates varying delays and facilitates lateral inhibition through the use of complex synaptic interconnections. In particular, these complex synaptic interconnections form the basis of receptive fields of which various types have been identified (Hosoya, et al., 2005). Simple on-off centre-surround receptive fields have been identified that respond to contrast change (Hosoya, et al., 2005), and to sharpen the image in space and also in time. Other types of receptive fields have been identified (Hosoya, et al., 2005, Kandel and Shwartz, 1981) where each type responds to different stimuli, for example orientated features. In addition, Shapley and Tolhurst (Shapley and Tolhurst, 1973) illustrated through psychophysical experiments that particular features, specifically edges, contours and corners are very important for visual perception (Shapley and Tolhurst, 1973). Thus, with the biological and psychophysical evidence indicating such a strong focus on the detection of specific features in biological vision systems, then surely artificial vision systems should take a similar approach?

In terms of image processing, a local feature may be regarded as an image pattern which differs from its immediate neighbourhood. Normally this difference is connected to a change of image property such as intensity, colour or texture. Commonly extracted features from images include edges, corners or interest points. Once features have been identified a region surrounding the feature is normally used to identify the feature with a descriptor which may be used for various applications. The image processing community has proposed many feature detection operators in the past 30 years, in particular a number of different approaches for the detection of edge features have been proposed. Some of the earliest methods of enhancing edges in images used small convolution masks to approximate the first derivative of the image intensities to enhance edges (Prewitt, 1970). Marr and Hildreth (Marr and Hildreth, 1980), used of zero crossings of the Laplacian of a Gaussian (LoG). Canny developed a multi-stage approach by incorporating first derivative approximation, non-maximal suppression and hysteresis suppression. Alternative feature detectors to detect edge junctions and corners have been proposed. Moravec (Moravec, 1977) developed a corner detector that shifted a small square window in vertical, horizontal, and diagonal directions. Harris and Stephens (Harris and Stephens, 1988) expanded the Moravec operator, removing the limitation of discrete window shifts, to develop a combined corner and edge detector. The operator response determines whether the detected feature is a corner, edge, or a flat region. Smith and Brady's SUSAN corner detector (Smith and Brady, 1997) is based on brightness comparisons over neighbourhoods and the detector can distinguish between corner and edge pixels. Shen and Wang (Shen and Wang, 2001) have expanded a local edge detector so that corners may also be detected. A combined edge and corner detector was presented in (Coleman et al., 2007) that was capable of detecting both feature types concurrently.

Whilst these techniques have been somewhat successful for the detection of particular features in images, when comparisons are drawn between the performance of such artificial vision feature detectors and the processing capabilities of biological vision systems it becomes apparent that current computer vision approaches suffer serious weaknesses. To try to overcome these failings of conventional artificial vision techniques research has started to examine, take inspiration, and emulate aspects of biological vision systems. This process of simulating biological information processing in engineering is termed neuro-engineering (O'Connor, et al., 2008) and such techniques are typically used for various artificial intelligent systems. For example, in (Wurtz and Lourens, 1999) a feedforward second generation neural network is used to detect corner points using a model of end-stopped cortical cells and corner features are extracted using Gabor filter responses in (Lüdtke, et al., 2002). In (GoodFellow, et al., 2012) a model that discovered characteristic features spontaneously was introduced; this differs from the work presented here in that we pre-define the feature detection structures taking inspiration from retinal circuitry. However, as precise knowledge of the complete retinal and cortex neuronal circuits is still not available, it is difficult to implement detailed exact models of biological visual processing. Thus, most current artificial models are based on specific assumptions, and simplified biological processes using variations of second generation neural networks that lack aspects of biological realism (Egmont, et al., 2003).

Spiking neural networks (SNNs) are the third generation class of neural networks that use a temporal coding scheme. This coding scheme enables spiking neural networks to more accurately mimic the biological information processing in the brain and visual system, and can be used to increase computational processing power and speed when compared with traditional second generation neural networks enabling real-time processing (Kunkle and Merrigan, 2002). SNNs use simple neuronal models and communicate using spikes in a manner similar to action potentials found in biological neurons. There has been some research investigating the application of SNNs to visual processing. In

(Van Rullen and Thorpe, 2002) scene categorisation is performed and this work is then expanded in (Masquelier and Thorpe, 2010) to perform object recognition. In (Hugues, et al., 2002) contours are detected in images through the synchronisation of integrate and fire neurons. SNN approaches have also recently been applied for the purpose of image segmentation, in (Wu, et al., 2007) which has proven to be fast and efficient and in (Wu, et al., 2007, Wu, et al., 2012) a SNN was proposed that detected right angle corners.

A SNN is used to model two areas of the brain concerned with motion with the aim of performing action recognition (Escobar, et al., 2009) and a distributed SNN is proposed for extracting saliencies in an image (Chevallier, et al., 2006). In (Chevallier and Dahdouh, 2009) a SNN is used to perform Difference of Gaussian filtering. Additionally, spiking neural networks have been previously used as controllers in evolutionary robotics to perform vision based obstacle avoidance (Floreano and Mattiussi, 2001), and for laser-based retinal model robot vision (Masuta and Kubota, 2008). In (Gamez, 2007, Lazdins, et al., 2011) a robot's sensory information is converted into spikes and a spiking neural network is used to process the information and control the robot. A biologically inspired flying robot is developed in (Floreano, et al. 2005) that uses a spiking neural network to convert visual information into motor commands and in (Hagras, et al., 2004) a spiking neural network is used to control a mobile robot using sonar sensors.

This paper presents an approach to feature detection using biologically inspired spiking neural networks to develop an artificial vision system that reflects a stronger correlation with biological visual systems than second generation neural networks. This stronger correlation is achieved via the use of a spiking neural network that mimics the biological visual processing system and the use of biologically plausible receptive field structures. The primary objective of this research is on the simultaneous processing and extraction of features from intensity images using biologically inspired techniques. By taking inspiration from traditional approaches to artificial visual feature detection and the real processes that take place in biological systems, the experimental work presented here aims to close the gap between these approaches. The aim is not to create an exact biological model of visual processing, rather to explore the use of specific biological processes in an artificial vision system for the extraction of image features that may be used for image matching purposes. The objective is to develop robust detection algorithms for artificial vision applications which can operate in the demanding visual conditions that biological systems operate within on a day-to-day basis, whilst supporting traditional feature matching algorithms. Visual processing is commonly represented using a feed-forward network, and here the presented approach will utilise a feed-forward spiking neural network. The spiking neural network discussed in this paper implements a number of biologically inspired visual processes including on-off receptive fields, orientation specific receptive fields, end-stopped receptive fields, specific synaptic connectivity and pooling of neuronal responses.

3. MODEL IMPLEMENTATION

Biological vision systems are normally described using a hierarchical processing model based on the types of cells outlined in the following sub-sections (Hubel and Wiesel, 2005). Light is detected by the photoreceptors within the retina, the signals are processed through the various retinal layers and retinal ganglion cells feed their output (in the form of action potentials) to the lateral geniculate nucleus and onto the visual cortex. The neurons within the retina and lateral geniculate nucleus form centre-surround receptive fields so the neurons respond strongly to contrast changes. By combining the responses from these cells, orientation specific cells may detect features of specific shape and orientation. The simple cells in turn feed into complex cells that detect even more complex features.

The operations involved in these biological processes are summation of outputs and nonlinearities, and as such may be modelled using a spiking neural network.

3.1 SPIKING NEURON MODELS

Biological neurons use short and sudden increases in voltage (commonly known as action potentials, spikes or pulses) to send information. The first scientific model of a spiking neuron, proposed by Hodgkin and Huxley (Hodgkin and Huxley, 1952), is based on experimental recordings from the giant squid axon using a voltage clamp method. The complexity in simulating this biologically realistic model is very high due to the number of differential equations and the large number of parameters. Thus, most computer simulations choose to use a simplified neuron model such as the integrate-and-fire model (I&F), leaky I&F model, conductance-based I&F or Izhikevich's model. The I&F model simulates the state of the neuron by its membrane potential, which receives excitatory or inhibitory signals from synaptic inputs from other neurons. Each input is weighted by its associated synaptic strength. The leaky I&F model produces a more biologically realistic neuron model adding a "leak" term to the membrane potential, reflecting the diffusion of ions that occurs through the membrane when some equilibrium is not reached in the cell. A full review of the biological behaviour of single neurons can be found in (Gerstner and Kistler, 2002) and a comparison of different neuron models can be found in (Izhikevich, 2004).

For implementation purposes the conductance-based I&F model has been selected to model the network neurons in this work. This model offers similar neuron behaviour to the Hodgkin-Huxley whilst providing a reduction in computational complexity. In the conductance-based I&F model the membrane potential $v(t)$ is governed by the following equation:

$$c_m \frac{dv(t)}{dt} = g_l (E_l - v(t)) + \frac{w_{ex} g_{ex}(t)}{A_{ex}} (E_{ex} - v(t)) + \frac{w_{ih} g_{ih}(t)}{A_{ih}} (E_{ih} - v(t)) \quad (1)$$

where c_m is the membrane capacitance, E_l is the membrane reversal potential, g_l is the conductance of the membrane, E_{ex} and E_{ih} are the reversal potential of the excitatory and inhibitory synapses respectively, w_{ex} and w_{ih} are weights for excitatory and inhibitory synapses respectively, A_{ex} and A_{ih} are the membrane surface areas connected to the excitatory and inhibitory synapses respectively. If the membrane potential $v(t)$ exceeds the threshold voltage v_{th} an action potential is generated and then $v(t)$ is reset to v_{reset} for a time τ_{ref} which is called the *refractory duration*. For simplicity τ_{ref} is set to 0 in this work. The variables $g_{ex}(t)$ and $g_{ih}(t)$ represent the conductance's of excitatory and inhibitory synapses respectively, which vary with time. The parameters of spiking neurons are based on data from real biological neurons (Wu, et al., 2013, Gerstner and Kistler, 2002). The following values of parameters are set for all the spiking neurons, $v_{th} = -60\text{mV}$, $v_{reset} = -70\text{mV}$, $E_{ex} = 0\text{mV}$, $E_{ih} = -75\text{mV}$, $E_l = -70\text{mV}$, $g_{ih} = 1.0\mu\text{S}/\text{mm}^2$, $g_{ex} = 1.0\mu\text{S}/\text{mm}^2$, $c_m = 10\text{nF}/\text{mm}^2$, $A_{ex} = 0.014103\text{mm}^2$, $A_{ih} = 0.02893\text{mm}^2$. The output spike train is then represented by a series of 1's or 0's representing whether or not a neuron fires at time t , i.e. $[S_{out}(t_1), S_{out}(t_2), \dots, S_{out}(t_M)]$.

3.2 RECEPTIVE FIELDS

In a biological system a receptive field is where a neuron integrates the signals from a group of afferent neurons. The receptive field of neurons in the visual system comprise of a 2-D region in visual space with varying size. Receptive fields form the basis of many aspects of the visual system and they have been observed in all areas of the visual system, from the retina to the visual cortex. A representation of a receptive field is illustrated in Figure 1 where the (green coloured) postsynaptic neuron has a receptive field formed by the (blue coloured) presynaptic nine neuron array. In this example each neuron in the receptive field connects to postsynaptic neuron through both excitatory and inhibitory synapses indicated by the red and black lines.

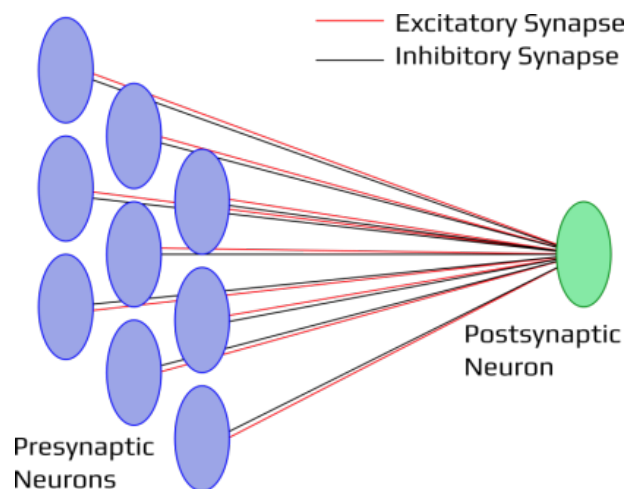


Figure 1: Receptive field of a spiking neuron. The (green coloured) postsynaptic neuron has a receptive field formed by the (blue coloured) presynaptic 9 neuron array. In this example each neuron in the receptive field connects to postsynaptic neuron through both excitatory (red) and inhibitory (black) synapses.

Various types of receptive fields have been observed experimentally. Some receptive fields have circular excitatory central regions and a larger surrounding circular inhibitory region and respond strongly to changes in contrast. Some receptive fields are elongated with an excitatory central oval and an inhibitory surrounding region and respond strongly to edges of particular orientations. Some receptive fields are rectangular, with one long side being excitatory and the other being inhibitory. The incoming light pattern needed to stimulate these receptive fields must have a particular orientation in order to excite the cell and produce an action potential. In the experimental work presented in this paper various types of receptive fields are used.

3.2.1 Centre-surround receptive fields

Many retinal ganglion cells have approximately circular receptive fields with distinct central and peripheral regions (called centre and surround). Figure 2 illustrates an example of the specific cells and synapses within the retina that may form such a receptive field.

There are two main types of centre-surround receptive fields: on-centre receptive fields respond best to light falling on the centre, and darkness falling on the surround; off-centre receptive fields respond best to darkness on the centre and light on the surround. In the case of both types of cell illumination of both the centre and surround regions receptive field produces a weak response. The result of the centre-surround architecture is that ganglion cells respond most strongly to spatial changes in contrast, such as the edges of an object. Figure 3 illustrates how an on-centre off-surround receptive field responds to stimulus. Shading indicates the area stimulated with light. The response to the stimulus is indicated below each receptive field. The largest response occurs when the entire excitatory area is illuminated, as illustrated in (b). Increasing the stimulus size further causes a decrease in firing due to centre-surround antagonism.

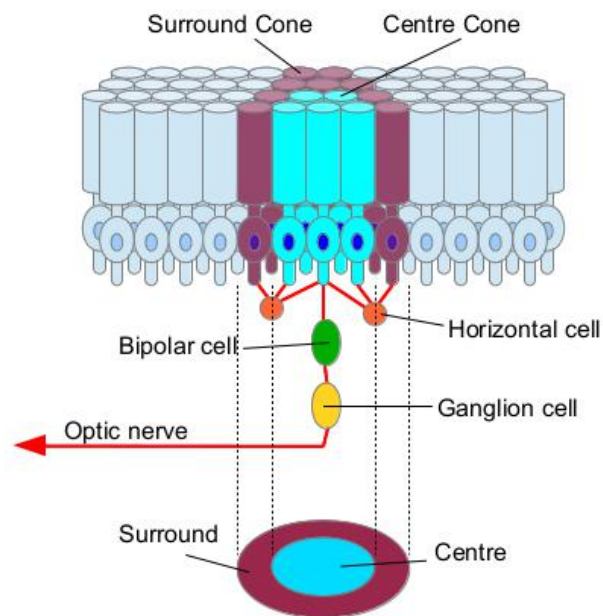


Figure 2. Centre-surround receptive fields are formed from a pool of photoreceptors. The photoreceptors can either act to excite (blue) or to inhibit (purple) a downstream bipolar cell. In this example the centre is excited thus this is an on-centre cell.

(a) (b) (c) (d)

Figure 3. Response of an on-centre (excitatory) off-surround (inhibitory) receptive field as the stimulus size is increased. Shading indicates the area stimulated with light. (Adapted from Hubel and Wiesel, 1961).

The difference-of-Gaussian model was used by (Rodieck, 1965) and (Enroth-Cugell and Robson, 1966) to demonstrate that the spatial centre-surround opposition could be well approximated with this filter. In the visual model proposed in this paper the difference of Gaussians model is used to implement the first stage in the model, replicating the processing stage between the photoreceptors and the retinal ganglion cells in order to detect contrast changes in the visual scene. The Laplacian-of-Gaussian model was proposed by Marr and Hildreth (Marr and Hildreth, 1980) and uses the second spatial-derivative of a Gaussian to model the receptive field shape. It also captures reasonably well the “Mexican hat” shape of retinal ganglion cell receptive fields and may be used as an alternative.

3.2.2 Orientation specific receptive fields

Orientation specific receptive fields were first discovered in the visual cortex by (Hubel and Wiesel, 1977) and described as *simple cells*. The receptive field is formed from elongated on and off sub-regions, with the spatial arrangement of the regions determining the neuron response to stimuli. It was proposed that each orientation specific cell gets its input from an array of centre-surround receptive fields with their centres forming a straight line, as illustrated in Figure 4. These properties make orientation specific receptive fields respond strongly to a line or edge stimulus with a specific orientation as illustrated in Figure 5.

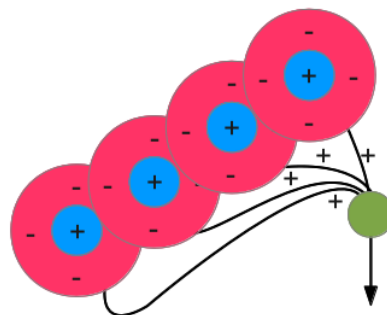


Figure 4. Hierarchical integration of neurons generates increasingly complex receptive field properties (Hubel and Wiesel, 1962). Orientation tuning of a neuron is achieved by integrating concentric receptive fields arranged in a linear array. The optimum stimulus now is a line of the correct orientation.

(a) (b) (c)

Figure 5. The receptive fields of orientation specific neurons are not circular, but rectangular. They respond especially well to rays of light that are oriented in a particular direction. These rectangular

receptive fields often have an ON centre band that responds positively to light, with two OFF side bands that respond to darkness. The diagram here shows that (a) when the beam of light is not present the cell does not respond, (b) when the beam of light is correctly orientated with the ON band the cell responds strongly, and (c) when the beam of light is not oriented to follow the ON band precisely, the cell responds weakly as the stimulus is simply not effective for this cell.

The most common mathematical function used to model response of orientation specific cells is a two dimensional Gabor functions (Gabor, 1946, Jones and Palmer, 1987). Gabor functions are used in this work to construct the weights for the receptive fields for the model second stage that detects lines of particular orientations.

3.2.3 End-stopped cells

End-stopped cells were first discovered by Hubel and Wiesel (Hubel and Wiesel, 1977) and described as *hyper-complex cells*. These cells respond strongly to edges or bars that terminate within their receptive field. Hubel and Wiesel identified two types, single end-stopped cells that respond strongly to line-ends and double end-stopped cells that respond strongly to very short line segments or small spots, circular objects or blobs. The behaviour of an end-stopped cell is illustrated in Figure 6.

(a) (b) (c)

Figure 6. End-stopped cell exhibiting length summation behaviour. The longer the stimulus line, the better is the response, but only until the line is as long as the receptive field. In (a) light falling on part of the excitatory region results in the neuron responding weakly. In (b) the stimulus is at the optimum size for the excitatory region resulting in the neuron responding strongly to the stimulus. In (c) the limit of the receptive field has been exceeded in both directions and as a result the neuron responds with a weaker response. The region from which responses are evoked is the activating region and the regions at either one or both ends is the inhibitory region. The total receptive field is made up of the activating region and the inhibitory region or regions at the ends.

The receptive field structure of end-stopped cells makes them especially sensitive to corners, curvature and terminators. The neuronal behaviour of end-stopped cells, centre-surround receptive fields and orientated receptive fields is of particular interest for the purposes of feature detection. By using combinations of these receptive fields it is possible to extract increasingly complex features, for example edges, orientated edges, endings of edges, and the junction of multiple edge endings, i.e. corners.

3.3 NETWORK IMPLEMENTATION

A hierarchical visual model that detects increasingly complex features using nonlinearities and summation operations may be modelled using a spiking neural network. This type of visual model has strong links with biological vision systems (Hubel and Wiesel, 2005, Rodriguez-Sanchez and Tsotsos, 2012) and forms the basis for the architecture presented here. The main contributions of this work are in the proposed spiking neural network structure, consisting of four processing layers corresponding to an edge detection layer, an orientation detection layer, an end-stopped detection layer, an interest point detection layer and in the way the different biologically inspired receptive field structures are used within the network in a biologically plausible manner (Hubel and Wiesel, 2005, Rodriguez-Sanchez and Tsotsos, 2012). This work builds upon our previous work on feature extraction using spiking neural networks (Kerr, et al., 2011b, 2012, 2013), the work of Wu (Wu, et al., 2012) and our previous work on image feature extraction (Kerr, et al., 2011a) but now we focus on modelling each

stage of the network using different receptive fields. The network model was implemented in the Python programming language with the Brian spiking neural simulator (Goodman and Brette, 2009) using a standard conductance based I&F model with parameters that are consistent with biological neurons (Gerstner and Kistler, 2002).

The network structure is illustrated in Figure 7. There is one array of neurons in the edge detection layer, Figure 7(b), with the same dimensions as the input image. For visual clarity only one neuron in this layer has been illustrated, with the associated receptive field for that neuron. The neuron is connected to the input layer via a centre surround receptive field with synaptic weights computed using a difference of Gaussian filter. There are four arrays of neurons in the orientation detection layer, Figure 7(c), each with the same dimensions as the input image. Again, for visual clarity on one neuron from each array has been illustrated. Each neuron in the orientation detection layer is connected to the corresponding neuron in the edge detection layer via an orientation specific receptive field with synaptic weights computed using Gabor filters. Each orientation specific array performs the processing for a different edge direction, in this case horizontal, vertical, and both diagonal directions. There are eight arrays of neurons in the end-stopped detection layer, Figure 7(d), again each with the same dimensions as the input image. Pairs of neurons in the end-stopped detection layer are connected to a corresponding neuron in the orientation detection layer via a receptive field constructed from excitatory and inhibitory connections. For example, the vertical orientation neuron is connected to two end-stopped neurons that detect edge features that have stopped at either the top or bottom of each receptive field. In the interest point detection layer, Figure 7(e), neuronal responses from the end-stopped layers are pooled through a receptive field with specific synaptic weights to enable the neuron to elicit a response in the presence of two or more end-stopped features. Each layer will now be discussed in detail in the following subsections.

(a) (b) (c) (d) (e)

Figure 7: Spiking Neural Network Structure with (a) one input layer and four processing layers corresponding to (b) edge detection layer, (c) orientation detection layer, (d) end-stopped detection layer and (e) interest point detection layer.

3.3.1 Edge detection layer

The first processing layer in the network represents the visual processing taking place within the retina. This layer uses an intensity image as input and produces a resulting spiking output. This corresponds to retina level processing where the photoreceptors detect external light stimulus and the retinal ganglion cells produce a spiking output. The input image is filtered using the difference of Gaussian technique to replicate the On-Centre Off-Surround and Off-Centre On-Surround ganglion cells found in the retina. Blurred versions of the input image are obtained by convolving the original grayscale image with Gaussian kernels having different standard deviations. Since the circularly symmetric Gaussian distribution $g(x, y)$ with two variables and standard deviation σ is

$$g(x, y) = \frac{1}{2\pi\sigma^2} e^{-\left(\frac{x^2+y^2}{2\sigma^2}\right)} \quad (2)$$

the difference of Gaussian filter can be calculated by

$$dog(x, y) = \frac{1}{2\pi\sigma_s^2} e^{-\left(\frac{x^2+y^2}{2\sigma_s^2}\right)} - \frac{1}{2\pi\sigma_c^2} e^{-\left(\frac{x^2+y^2}{2\sigma_c^2}\right)} \quad (3)$$

where the parameters σ_s and σ_c are the standard deviations of the surround and centre elements of the difference of Gaussian filter. The following ratio between standard deviations was used

$$\frac{\sigma_c}{\sigma_s} = 1.6 \quad (4)$$

to ensure the difference of Gaussian filter approximates the receptive fields of biological ganglion cells (Marr and Hildreth, 1980). The filter is illustrated in Figure 8.

(a) 3D plot of difference of Gaussian filter

(b) Visual representation of receptive field weights

Figure 8. Plot of difference of Gaussian filter used to construct receptive field synaptic weights in edge detection layer

The difference of Gaussian response for each image pixel is then converted into a resulting spike train where high responses correspond to spike trains with short delays and low responses correspond to spike trains with long delays. Thus, the highest spiking output from the difference of Gaussian filter are areas where the image intensity changes rapidly, corresponding to the most rapidly firing neuron. Zero or negative DoG responses are areas where the image intensity remains constant corresponding to the slowest firing neurons.

3.3.2 Orientation detection layer

Detection of edge and line segments of a particular orientation is an important preliminary stage in corner detection. The second layer in the network represents the orientation specific visual processing taking place within the simple cells in the visual cortex. To implement the orientation specific neurons, receptive fields are formed with weights determined using Gabor filters. The responses of even and odd simple cells may be modelled using the real and imaginary parts of a Gabor function,

$$G_{\sigma,\theta}(x, y) = \exp\left(i \frac{\pi}{\sqrt{2}\sigma} (x \cos \theta + y \sin \theta)\right) \exp\left(-\frac{x^2 + y^2}{2\sigma^2}\right) \quad (5)$$

where σ is the width of the receptive field and θ denotes the preferred orientation of the cell. Here we set $\sigma = 10$ to be consistent with the work presented in (Rao and Ballard, 1999) where simple cell receptive fields were modelled using Gabor functions. The Gabor filters are used to construct four types of neuron with receptive fields that respond strongly to line segments with horizontal, vertical and both diagonal orientations as illustrated in Figure 9 and Figure 10.

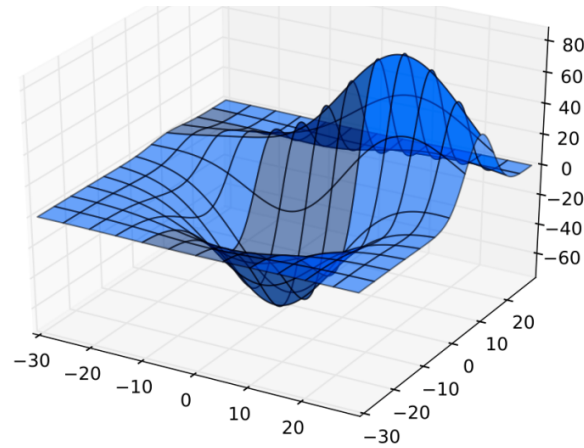


Figure 9. 3D plot of Gabor filter used to construct synaptic weights for receptive fields in orientation detection layer

(a) Horizontal edge receptive field weights (b) Vertical edge receptive field weights (c) Diagonal-*a* edge receptive field weights (d) Diagonal-*b* edge receptive field weights

Figure 10. Visual representation of Gabor filters used to construct synaptic weights for receptive fields in orientation detection layer. Each orientation specific receptive field performs the processing for a different edge direction, in this case (a) horizontal, (b) vertical, and (c & d) both diagonal directions.

3.3.3 End-stopped detection layer

Detection of edge and line segments that correspond to the end of a segment is the next important stage in corner detection. The third layer in the network represents the response of single end-stopped cells found within the hyper-complex cells in the visual system. These cells are modelled as receptive fields with four excitatory and one inhibitory neuron. There are eight arrays of neurons in the end-stopped detection layer, modelled as receptive fields with specific excitatory and inhibitory regions and illustrated in Figure 11. Pairs of neurons in the end-stopped detection layer are connected to a corresponding neuron in the orientation detection layer via a receptive field constructed from excitatory and inhibitory connections. For example, the neuron in the orientation detection layer with the horizontal oriented receptive field (Figure 10(a)), is connected to two corresponding end-stopped neurons (Figure 11(a) and Figure 11(b)) that detect edge features that have stopped at either the left or right of each receptive field.

(a) Left-stop (b) Right-stop (c) Top-stop (d) Bottom-stop
(e) Right-top-stop (f) Left-bottom-stop (g) Left-top-stop (h) Right-bottom-stop

Figure 11. Visual representation of end-stopped neuronal receptive fields used to construct synaptic weights for receptive fields in end-stopped detection layer. Each end-stopped receptive field performs the processing for a different end edge segments.

3.3.4 Interest point detection layer

The interest point layer determines the presence of an interest point through pooling of the neuronal responses from the end-stopped detection layer. Using a 5x5 receptive field the presence of two or more strongly firing end-stopped neurons firing indicates the presence of an interest point by activating the associated interest point neuron. The interest point neuron firing map indicates those neurons that have reached each individual neuron's firing threshold and thus produced a spike. Hence, an interest point is detected at a location where a neuron in the interest point detection layer has fired at least one spike.

4. EXPERIMENTAL EVALUATION

In order to test the performance of our proposed spiking neural network we first construct a synthetic image with two rectangular shapes at different orientations. The image intensities used to construct the step edges in the synthetic image are 100, 129, and 158 (where the possible range of intensities is [0-255]) and the image size is 45x45 pixels. In the case of the orientated rectangle shape the intensities are obtained through bilinear interpolation using the same step edge intensities. The synthetic image is then used as input into the spiking neural network. The output from the strongly firing interest point detection neurons are transformed into image locations and indicated by highlighting with a rectangular region in Figure 12.

(a) Example synthetic input image

(b) Example network output

Figure 12. (a) Synthetic image with two rectangular shapes at different orientations used as input to the network and (b) output from the strongly firing interest point detection neurons are transformed into image locations and indicated by highlighting with a rectangular region.

We have also applied the network to a simple real image to examine its performance in comparison to the standard corner detection algorithm of Harris and Stephens (Harris and Stephens, 1988), as illustrated in Figure 13. This visual comparison illustrates the SNN provides similar results to the Harris corner detector.

(a) Spiking Neural Network interest point outputs

(b) Harris corner detector interest point outputs

Figure 13. Results of interest point detection on real image

Performance evaluation of the spiking neural network interest point detector was conducted using the set of test images and testing software provided by the collaborative work between *Katholieke Universiteit Leuven*, *Inria Rhone-Alpes*, *Visual Geometry Group* and the *Center for Machine Perception*. The images and testing software are available for public download³. A subset of the test images used in this evaluation are illustrated in Figure 14.

(a) Scale change –original

(b) Scale change – 1.35 zoom

(c) Scale change – 2.8 zoom

(d) Decreasing light - original

(e) Decreasing light - f3

(f) Decreasing light - f6

³ <http://www.robots.ox.ac.uk/~vgg/research/affine>

(g) JPEG compression - original (h) JPEG compression – 80% (i) JPEG compression – 97.5%
(j) Viewpoint angle - original (k) Viewpoint angle – 30 degrees (l) Viewpoint angle – 60 degrees

Figure 14. Subset from the four test sequences used to test performance with respect to scale and rotation invariance, illumination change, JPEG compression, and viewpoint change. Each sequence contains six images in total but only three from each sequence are included in this figure.

In the evaluation we use four test sequences from the dataset to test performance with respect to scale and rotation invariance, illumination change, JPEG compression, and viewpoint change. Each sequence contains six images, an original image of the scene and five images with progressively different changes. In the viewpoint change test sequence the camera varies from a fronto-parallel view to one with significant foreshortening at approximately 60 degrees to the camera. The scale and rotation change test sequences are acquired by varying the camera zoom and focus respectively. The scale changes by approximately a factor of four. The illumination changes are introduced by varying the camera aperture. The JPEG sequence is generated using a standard image browser with the image quality parameter varying from 40% to 2%. In all cases the images are related by homographies meaning that the mapping relating images is known and this mapping is used to determine ground truth matches for the interest point detectors.

In the evaluation, the Harris and Stephens (Harris and Stephens, 1988) corner detector, the SURF interest point detector (Bay, 2006), and the FESID interest point detector (Kerr, 2011a) are used for comparisons with the spiking neural network feature detector. Whilst other feature detectors are available the Harris detector was specifically chosen as it also operates at a single image scale in a manner similar to the proposed spiking network detector. In addition we have also included the scale and rotationally invariant SURF and FESID interest point detectors. These detectors are included to provide a benchmark with computer vision methods although it should be noted that they lack biological plausibility. A full evaluation of different computer vision interest point detectors using the same software and images has been carried out in (Mikolajczyk, et al., 2005) and (Bay, et al., 2007) and the reader is referred to this work for full details.

In order to assess the performance of an interest point detector with respect to matching, two important aspects need to be considered (a) the repeatability of the interest points, such as the average number of corresponding points detected in images under different transformations, both in absolute and relative terms and (b) the accuracy of localisation and interest point estimation. The repeatability metric explicitly compares the geometrical stability of detected interest points between different images of a scene under different viewing conditions. Between two images the *repeatability rate* is defined as the percentage of the total interest points that are detected in both images considering only the part of the scene that is common to both images. In general for matching features between images we would like a detector to have a high repeatability score and a large number of correspondences.

It is important to consider only the parts of the scene that are visible in both images because if an object is visible in one image but not the other, the interest points detected for that object could never correspond. When determining whether an interest point in one image corresponds to another interest point in a second image it is not appropriate to just measure the distance between them, as the measure needs to be the same for points detected at all scales. Interest points are determined to correspond if the error in pixel location is less than 1.5 pixels and the overlap error, determined by a region around the interest point, is less than a pre-defined threshold.

In the evaluation performed here we use a circular region with a single fixed diameter to compute the interest point descriptor, because both the spiking neural network interest point detector and the Harris corner detector are not scale invariant. When an image pair has a non-uniform scaling, the circular region may transform to an ellipse. The region that is common to both ellipses is the overlap region. The overlap is measured based on the ratio of intersection and union of the ellipses. If two regions have perfect overlap the ratio would be 1, and for two regions with no overlap the ratio would be 0. Thus, where the error in pixel location is less than 1.5 pixels, and the overlap error is below 60%, similar to the evaluation of the SURF detector (Bay, et al., 2006), the interest points are deemed to correspond. The purpose of measuring the overlap is that when regions are matched in different images, robust descriptors help to match the features that do not correspond directly. Some previous evaluations have also used an overlap as low as 40%, but even when the overlap is 60% robust descriptors should still be able to correctly match the regions (Bay, et al., 2006). For full information on how the detected regions are measured the reader is referred to (Mikolajczyk, et al., 2005).

The first image sequence to be evaluated is the scale and rotation change sequence and the results are presented in Figure 15. Here the SNN model detects quite a large amount of corresponding regions when compared with the Harris corner detector. Performance for both the SNN model and Harris corner detectors falls rapidly due to the scale change as these detectors are not scale invariant. Examining the repeatability rate (i.e. percentage wise) the SNN model performs similar to the Harris detector but performance is slightly reduced. It is presumed that this is due to the fact that the SNN model edge orientations are detected in discrete directions (i.e. the detector does not have an isotropic response) and is therefore not rotationally invariant. Performance could possibly be improved with respect to rotational invariance by increasing the number of orientation detection neurons and associated receptive fields. The SURF and FESID detectors perform much better as these detectors are designed to be scale and rotationally invariant and represented current state-of-art detectors in the computer vision community.

(a) Number of corresponding interest points in absolute terms

(b) Repeatability rate of detector – number of interest points in relative terms

Figure 15. Comparison of Spiking Neural Network Feature Detector and Harris corner detector using the scale and rotation image sequence in Figure 14 (a) – Figure 14 (c).

The second image sequence to be evaluated is the illumination change sequence and the results are presented in Figure 16. Here the performance of the SNN model is lower than the Harris corner detector, both in absolute and relative terms. This indicates that the SNN model is particularly sensitive to illumination change. This poor response to global illumination change is entirely expected as it is well known that centre-surround receptive fields do not respond very well to global illumination changes (Heckenlively and Arden, 2006), hence the poor repeatability response. However, the SURF and FESID interest point detectors use a local binary pattern type features that result in a detector providing invariance to global illumination change. The incorporation of global light adaptation mechanisms such as those found in the retina (Bartlett, 1965) would improve this aspect of the SNN model but are currently beyond the scope of the work presented here.

(a) Number of corresponding interest points in absolute terms

(b) Repeatability rate of detector – number of interest points in relative terms

Figure 16. Comparison of Spiking Neural Network Feature Detector and Harris corner detector using the illumination change image sequence in Figure 14 (d) – Figure 14 (f).

The third image sequence to be evaluated is the JPEG compression change sequence and the results are presented in Figure 17. Here the SNN models performance is much improved over the Harris detector, SURF detector and FESID detector. In the case of repeatability all the detectors perform similarly.

(a) Number of corresponding interest points in absolute terms

(b) Repeatability rate of detector – number of interest points in relative terms

Figure 17. Comparison of Spiking Neural Network Feature Detector and Harris corner detector using the JPEG compression change image sequence in Figure 14 (g) – Figure 14 (i).

The final image sequence to be evaluated is the viewpoint angle change sequence and the results are presented in Figure 18. The viewpoint change sequence is generally considered to be the most difficult evaluation sequence. Here the SNN model detects quite a large amount of corresponding regions when compared with the other methods. Examining the repeatability rate (i.e. percentage wise) the SNN model performs poorer than the Harris detector but performance is increased as the viewpoint angle is increased. In the case of both the SNN model and the Harris detector performance rapidly decreases as the viewpoint angle is increased, mainly due to the fact that these detectors are not designed for rotational or scale invariance.

(a) Number of corresponding interest points in absolute terms

(b) Repeatability rate of detector – number of interest points in relative terms

Figure 18. Comparison of Spiking Neural Network Feature Detector and Harris corner detector using the viewpoint change image sequence in Figure 14 (j) – Figure 14 (l).

5. DISCUSSION AND FUTURE WORK

The spiking neural network presented in this paper is constructed using a hierarchical structure that is composed of spiking neurons with various receptive fields. The input image is converted to retinal ganglion cell output spike trains by convolving with difference of Gaussian filters. The spike trains are presented to the network and the various receptive fields process the image, performing edge detection, orientation detection, end-stopped detection and interest point detection. The spiking neuron models provide powerful functionality for integration of inputs and generation of spikes. Synapses are able to perform different complicated computations. This paper demonstrates how a spiking neural network can detect interest point features in an image. The performance illustrates that the proposed detector is comparable with the Harris corner detector but still falls behind some of the state-of-art interest point detectors with more challenging image transformations. Further work will involve the incorporation of more orientation detection neurons, incorporating scale invariance, and the incorporation of light adaptation mechanisms.

ACKNOWLEDGEMENTS

This work was supported by funding from the European Union Seventh Framework Programme (FP7-ICT-2011.9.11) under grant number [600954] ("VISUALISE").

REFERENCES

- Bay, H., Tuytelaars, T., and Van Gool, L. (2006). "Surf: Speeded up robust features." *Computer Vision–ECCV 2006*. Springer Berlin Heidelberg, 404-417.
- Bartlett NR. (1965). Dark and light adaptation. In: Graham CH, editor. *Vision and visual perception*. New York: John Wiley and Sons, Inc.
- Chevallier, S. and Dahdouh, S. (2009). Difference of Gaussians Type Neural Image Filtering with Spiking Neurons". *Proc. of Int. Conf. on Neural Computation, Maderia, Portugal*.
- Chevallier, S., Tarroux, P. and Paugam-Moisy, H. (2006). Saliency extraction with a distributed spiking neural network. *Proc. of ESANN*, 209-214.
- Coleman, S.A., Kerr, D., and Scotney, B.W. (2007) Concurrent Edge and Corner Detection. In: *IEEE International Conference on Image Processing (ICIP 2007)*, San Antonio, Texas. IEEE Signal Processing Society. V-273
- Egmont-Petersen, M., De Ridder, D. and Handels, H. (2002). Image processing with neural networks-a review. *Pattern Recognition*,35(10), 2279-2301.
- Enroth-Cugell C. and Robson J. G. (1966) The contrast sensitivity of retinal ganglion cells of the cat. *J. Physiol.* 187. 51775.52
- Escobar, M.J., Masson, G.S., Vieville, T., and Kornprobst, P. (2009). Action Recognition Using a Bio-Inspired Feedforward Spiking Network. *International Journal of Computer Vision*. 82, 3, 284-301.
- Floreano, D. and Mattiussi, C. (2001) Evolution of Spiking Neural Controllers for Autonomous Vision-based Robots. in *Evolutionary Robotics IV*, Berlin : Springer-Verlag, 2001
- Floreano, D., Zufferey, J.-C. and Nicoud, J.-D. (2005) From Wheels to Wings with Evolutionary Spiking Neurons. *Artificial Life*, 11(1-2) pp. 121-138.
- Gabor, D. (1946). Theory of communication. *J. Inst. Elec. Eng.*, 93, 429–457.
- Gamez, D. "SpikeStream: A Fast and Flexible Simulator of Spiking Neural Networks." *Proceedings of ICANN*. V.4668, pp. 370-379. *Lecture Notes in Computer Science*, Springer Verlag, 2007.
- Gerstner, W., Kistler, W. (2002). *Spiking Neuron Models: Single Neurons, Populations, Plasticity*", Cambridge University Press.
- Gollisch, T. and Meister, M. (2010) "Eye smarter than scientists believed: neural computations in circuits of the retina." *Neuron* 65.2 (2010): 150-164.
- Goodfellow, I.J., Courville, A. and Bengio, Y. (2012) "Spike-and-slab sparse coding for unsupervised feature discovery." *arXiv preprint arXiv:1201.3382* (2012).

- Goodman DF. and Brette R. (2009). The Brian simulator, *Front. Neurosci.* 3, 2, 192-197.
- Hagras, H., Pounds-Cornish, A., Colley, M., Callaghan, V., and Clarke, G. "Evolving spiking neural network controllers for autonomous robots." *Proceedings of IEEE International Conference on Robotics and Automation, (ICRA) 2004.*
- Harris, C., and Stephens, M. (1988). A Combined Corner and Edge Detector. *Proceedings 4th Alvey Vision Conf.* 147-151.
- Heckenhively, J. R., & Arden, G. B. (Eds.). (2006). *Principles and practice of clinical electrophysiology of vision.* MIT press.
- Hodgkin, A., Huxley, A. (1952). A quantitative description of membrane current and its application to conduction and excitation in nerve. *Journal of Physiology, London*, vol. 117, pp. 500-544.
- Hosoya, T., Baccus, S.A., Meister, M. (200). Dynamic predictive coding by the retina. *Nature*, vol. 436, pp. 71-77.
- Hubel, D.H. and Wiesel, T.N. (1977). Ferrier Lecture functional architecture of macaque visual cortex. *Proc. R. Soc. Lond. B.*, 198, 1–59.
- Hubel, D.H., and Wiesel, T.N. (2005). *Brain and visual perception: the story of a 25-year collaboration.* New York, New York: Oxford University Press.
- Hugues, E., Guilleux, F. and Rochel, O. (2002). Contour Detection by synchronization of Integrate and Fire Neurons. *LNCS.* 2525, 60-69.
- Izhikevich, E.M. (2004). Which model to use for cortical spiking neurons? *IEEE Trans. on Neural Networks*, vol. 15, no. 5.
- Izhikevich, E.M., Edelman, G.M. (2008). A Large-Scale Model of Mammalian Thalamocortical Systems. *Proc. National Academic Science, USA*, vol. 105, no. 9, pp.3593-3598.
- Jones, J. and Palmer, L. (1987). An evaluation of the two-dimensional gabor filter model of simple receptive fields in cat striate cortex. *Journal of Neurophysiology*, 58, 1233–1258.
- Kandel, E.R., Shwartz, J.H. (1981). *Principles of neural science.* Edward Arnold (Publishers) Ltd.
- Kerr, D, Coleman, SA and Scotney, BW (2011a) A Finite Element Blob Detector for Robust Features. In: 16th International Conference on Image Analysis and Processing, Ravenna, Italy. Springer. Vol 6978/2011
- Kerr, Dermot, et al. "Spiking Hierarchical Neural Network for Corner Detection." (2011b): In: *Int. Conf. on Neural Computation Theory and Applications*, Paris, France. SciTePress 230-235.
- Kerr, D, Coleman, SA, McGinnity, TM, Wu, Qingxiang and Clogenson, M. (2012) A novel approach to robot vision using a hexagonal grid and spiking neural networks. In: *The 2012 International Joint Conference on Neural Networks (IJCNN)*, Brisbane, Australia. IEEE.
- Kerr, D, Coleman, SA, McGinnity, TM and Clogenson, Marine (2013) Biologically Inspired Intensity and Range Image Feature Extraction. In: *The 2013 International Joint Conference on Neural Networks (IJCNN'13)*, Dallas, USA. IEEE

- Kunkle, D.R. and Merrigan, C. (2002). Pulsed neural networks and their application. Computer Science Dept., College of Computing and Information Sciences, Rochester Institute of Technology.
- Lazdins, L., Fidjeland, A.K., Gamez, D. "iSpike: A Spiking Neural Interface for the iCub Robot". , Proceedings of the International workshop on bio-inspired robots. 2011.
- Lüdtke, N., Luo, B., Hancock, E.R., Wilson, R.C. (2002). Corner Detection Using a Mixture Model of Edge Orientation. ICPR (2) 2002: 574-577
- Marr, D., Hildreth, E. (1980), Theory of Edge Detection, Proceedings of the Royal Society of London. Series B, Biological Sciences 207 (1167): 187–217, doi:10.1098/rspb.1980.0020
- Masquelier, T., and Thorpe, S.J. (2010). Learning to recognize objects using waves of spikes and Spike Timing-Dependent Plasticity. The 2010 International Joint Conference on Neural Networks (IJCNN). 1-8.
- Masuta, H., Kubota, N. "The perception for partner robot using spiking neural network in dynamic environment." SICE Annual Conference, 2008.
- Mikolajczyk, K., Tuytelaars, T., Schmid, C., Zisserman, A., Matas, J., Schaffalitzky, F., Kadir T., and Van Gool, L. (2005) A comparison of affine region detectors. In IJCV 65(1/2):43-72
- Moravec, H.P. (1977) Towards Automatic Visual Obstacle Avoidance. Proceedings 5th Int. Joint Conference. Artificial Intelligence. Cambridge, MA, USA. 584.
- O'Connor, D.H., Huber, D., and Svoboda, K. (2008). Reverse engineering the mouse brain. Nature 461, 923-929.
- Paugam-Moisy, H. and Bohte, S.M. (2009). Computing with spiking neuron networks. Handbook of Natural Computing. 40. Springer, Heidelberg.
- Prewitt, J.M.S. (1970) "Object Enhancement and Extraction" in "Picture processing and Psychopictorics", Academic Press.
- Rao, RPN, and Ballard, D. (1999) "Predictive coding in the visual cortex: a functional interpretation of some extra-classical receptive-field effects." Nature neuroscience 2.1 (1999): 79-87.
- Rodieck, R. W. (1965). Quantitative analysis of cat retinal ganglion cell response to visual system. Vision Research, 5, 583–601.
- Rodriguez-Sanchez, A.J., and Tsotsos, J.K. (2012). The roles of endstopped and curvature tuned computations in a hierarchical representation of 2D shape. PloS One, 7, 1-13.
- Shapley, R.M. and Tolhurst, D.J. (1973). Edge detectors in human vision. Journal of Physiology. 229, 1, 165-183
- Shen, F., and Wang, H. (2001). A Local Edge Detector Used for Finding Corners. Proceedings 3rd Int. Conf. Inf, Comm. And Signal Processing. Singapore.
- Smith, S.M., and Brady, J.M. (1997). SUSAN – A New Approach to Low Level Image Processing. IJCV. 23, 1, 45-78.

Van Rullen R, and Thorpe S. (2002). Surfing a spike wave down the ventral stream. *Vision Research*. 42, 2593-2615.

Wässle, H. (2004) Parallel processing in the mammalian retina. *Nat. Rev. Neurosci.* 5, 747-757.
<http://brain.mpg.de/research/emeriti/heinz-waessle/publications.html#sthash.BoHUUz8w.dpuf>

Wu, Q., McGinnity, M., Maguire, L., Belatreche, A., Glackin, B. (2007). Edge Detection Based on Spiking Neural Network Model. *Proc Int Conf on Intelligent Computing, LNAI 4682*, pp. 26–34, Springer-Verlag Berlin Heidelberg.

Wu, Q., McGinnity, T.M., Maguire, L., Cai, R., Chen, M. (2013). A visual attention model based on hierarchical spiking neural networks. *Neurocomputing*
<http://dx.doi.org/10.1016/j.neucom.2012.01.046>, 2012.

Wurtz, R.P. Lourens, T. (1999). Corner detection in color images through a multiscale combination of end-stopped cortical cells, *Image and Vision computing*, 1999.

Vitae

Dermot Kerr received a BSc(Hons) in Computing Science from the University of Ulster, UK in 2005, and a PhD in Computing and Engineering from the University of Ulster, UK in 2009. He is currently a research fellow in the School of Computing and Intelligent System at the University of Ulster, Magee. His current research interests are in mathematical image processing, feature detection, omnidirectional vision and robotics. Dr. Kerr is a member of the Irish Pattern Recognition and Classification Society.



Sonya Coleman received the Ph.D. degree from the University of Ulster Derry, Northern Ireland, in May 2003. She is currently a Senior Lecturer with the Faculty of Computing and Engineering, University of Ulster. She has authored more than 80 publications in her research area. Her current research interests include robotics, machine vision, digital image processing, and pattern recognition. Dr. Coleman is a member of the Irish Pattern Recognition and Classification Society and the London Mathematics Society.



Thomas Martin McGinnity (S'09–M'83) received the Degree (First Class Hons.) in physics and the Ph.D. degree from the University of Durham, Durham, U.K., in 1975 and 1979, respectively. He is a Professor of intelligent systems engineering with the Faculty of Computing and Engineering, University of Ulster, Derry, Northern Ireland. He is currently the Director of the Intelligent Systems Research Centre, which encompasses the research activities of approximately 100 researchers. Formerly, he was an Associate Dean of the Faculty and Director of the University's technology

transfer company, Innovation Ulster, and a spin out company Flex Language Services. He has authored or co-authored more than 275 research papers. His current research interests are focused on computational intelligence, and in particular on computational systems, which explore and model biological signal processing, specifically in relation to cognitive robotics and computation neuroscience. Prof. McGinnity was a recipient of the Senior Distinguished Research Fellowship and a Distinguished Learning Support Fellowship in recognition of his contribution to teaching and research. He is a fellow of the IET and Chartered Engineer.



Marine Clogenson was a visiting researcher at the University of Ulster. She is now Scientific Assistant at EPFL in Switzerland.

